Inorg. Chem. **2005**, *44*, 6314–6323

Non-Interpenetrating Transition Metal Diorganophosphate 2-Dimensional Rectangular Grids from Their 1-Dimensional Wires: Structural Transformations under Mild Conditions†

Ramasamy Pothiraja,‡ Malaichamy Sathiyendiran,‡ Ray J. Butcher,§ and Ramaswamy Murugavel*,‡

Departments of Chemistry, IIT-Bombay, Powai, Mumbai-400 076, India, and Howard University, Washington District of Columbia 20059

Received May 11, 2005

The manganese, cobalt, and cadmium complexes $[M(dtbp)_2]_n$ (M = Mn (**1**) and Co (**2**)) and $[Cd(dtbp)_2(H_2O)]_n$ (**3**) (dtbp = di-*tert*-butyl phosphate), which exist as one-dimensional molecular wires, transform to non-interpenetrating rectangular grids $[M(dtbp)_2(bpy)_2{\cdot}2H_2O]_n$ (M = Mn (**4**), Co (**5**), and Cd (**6**)) by the addition of 4,4-bipyridine (bpy) at room temperature. Products **4**–**6** have also been prepared by a room-temperature reaction or by solvothermal synthesis in methanol through a direct reaction between the metal acetate, di-*tert*-butyl phosphate, and 4,4′-bipyridine (bpy) in a 1:2:2 molar ratio. Single-crystal X-ray structure determination of **4**–**6** shows that these compounds are composed of octahedral transition metal ions woven into a two-dimensional grid structure with the help of bpy spacer ligands. The axial coordination sites at the metal are occupied by bulky unidentate dtbp ligands, which prevent any interpenetration of the individual grids. The change of reaction conditions from solvothermal to hydrothermal, for the attempted synthesis of a magnesium grid structure, however leads to the isolation of an organic phosphate $[(H_2bpy)(H_2PO_4)_2]$ (**7**) and an inorganic phosphate $[Mg(HPO_4)(OH_2)_3]$ (**8**). Compound **7** can also be prepared quantitatively from a direct reaction between bpy and H_3PO_4. The new organic phosphate **7** is a unique example of a phosphate material with alternating layers of $[H_2bpy]^{2+}$ cations and $[H_2PO_4]^-$ anions that are held together by hydrogen bonds. Solid-state thermal decomposition of **4**–**6** produced the respective metaphosphate materials $[M(PO_3)_2]$ (M = Mn (**9**), Co (**10**), and Cd (**11**)). All new metal–organic phosphates have been characterized by elemental analysis, thermal analysis (TGA, DTA, DSC), and IR and NMR spectroscopy. The metaphosphate ceramic materials were characterized by IR spectral and powder X-ray diffraction studies.

Introduction

Modern crystal engineering offers potential for the development of rational strategies for the design of new crystalline solids with functional properties.[1,2] For example, the specific network topology of a coordination polymer can be controlled by a careful selection of metal coordination geometry and organic *spacer* ligands. An elegant example of such a designed and largely predictable coordination polymeric network is exemplified by two-dimensional square or rectangular grids generated from square planar or octahedral metal ions and linear bifunctional spacer ligands such as 4,4′-bipyridine (bpy), resulting in compounds which have cavities suitable for either interpenetration or enclathration by a wide range of organic guest molecules.[3−7] It has been suggested that if the void created by the formation of a two-dimensional

* To whom correspondence should be addressed. E-mail: rmv@iitb.ac.in. Fax: +(22) 2572 3480.

† Dedicated to Professor S. Chandrasekaran on his 60th birthday.

‡ IIT-Bombay.

§ Howard University.

(1) (a) *Crystal Engineering: The Design and Applications of Functional Solids*; Seddon, K. R., Zaworotko, M. J., Eds.; NATO ASI Series; Kluwer Academic: Dordrecht, The Netherlands, 1998. (b) *Crystal Engineering: From Molecules and Crystals of Materials*; Braga, D., Grepioni, F., Orpen, A. G., Eds.; NATO ASI Series; Kluwer Academic: Dordrecht, The Netherlands, 1999.

(2) (a) Hagrman, P. J.; Hagrman, D.; Zubieta, J. *Angew. Chem., Int. Ed.* **1999**, *38*, 2638. (b) Yaghi, O. M.; Li, H.; Davis, C.; Richardson, D.; Groy, T. L. *Acc. Chem. Res.* **1998**, *31*, 474. (c) Batten, S. R.; Robson, R. *Angew. Chem., Int. Ed.* **1998**, *37*, 1460. (d) James, S. L. *Chem. Soc. Rev.* **2003**, *32*, 276.

(3) (a) Noro, S.; Kitagawa, S.; Kondo, M.; Seki, K. *Angew. Chem., Int. Ed.* **2000**, *39*, 2082. (b) Fu, A.; Huang, X.; Li, J.; Yuen, T.; Lin, C. L. *Chem.*—Eur. J. **2002**, *8*, 2239. (c) Tao, J.; Tong, M. L.; Chen, X. M. *J. Chem. Soc., Dalton Trans.* **2000**, 3669. (d) Ma, B. Q.; Gao, S.; Yi, T.; Xu, G. X. *Polyhedron* **2001**, *20*, 1255. (e) MacGillivray, L. R.; Subramanian, S.; Zaworotko, M. J. *J. Chem. Soc., Chem. Commun.* **1994**, 1325.

10.1021/ic050742z CCC: $30.25
Published on Web 08/06/2005

grid structure is more than 50% of the crystal volume,[4a] a considerable reduction in the volume of void takes place by simple interpenetration of the grid structures.[3−7] In this context, there have been some efforts in the literature to avoid this interpenetration in two-dimensional grids as well as other framework structures to have enough room for carrying our host−guest or clathration chemistry.[2d,8] However, no general methodologies have yet been developed to achieve this goal.

One of the major interests in metal phosphate chemistry is concerned with the structural transformations *under mild conditions*.[9] Although it has been suggested by Ozin et al. as early as in 1998 that it is possible to effect transformations among aluminophosphates,[10] only recent experiments have shown that it is indeed possible to convert a molecular aluminophosphate into either a two- or three-dimensional structure.[9] Rao et al. have recently shown that a zero-dimensional zinc phosphate could be transformed to ladder, layer, and three-dimensional structures,[11] apart from its unusual transformation to a sodalite type structure.[12] While a few examples of conversion of low-dimensional molecular phosphates to insoluble crystalline framework solids of higher dimensionality are known,[9] there are no known reports on the transformation of one form of an organic soluble molecular phosphate into another which is also accompanied by a change in the dimensionality.

Chart 1. Structural Diversity of Transition Metal Di-*tert*-butyl Phosphate Complexes

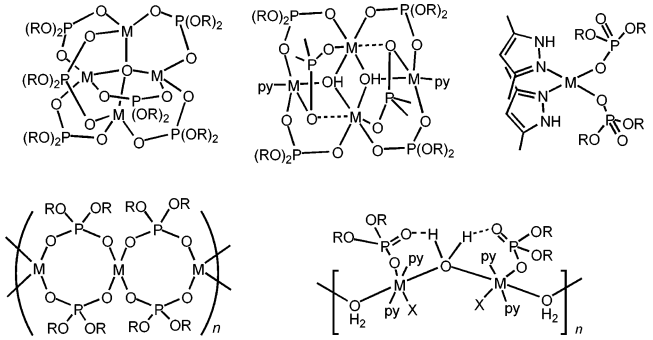

R = *t*Bu; M = a transition metal

The low-temperature thermolysis of single-source precursors for the preparation of materials with improved properties is gaining considerable attention in recent years owing to the ability of this method to provide atomic level control over the composition and homogeneity of the final material.[13] Recent studies reveal that di-*tert*-butyl phosphate (dtbp-H) could serve as an ideal starting material for the preparation of metal complexes that decompose neatly at *low temperatures* to yield fine particle metal phosphates.[14−21] For example, the decomposition behavior of these compounds probed by TGA and bulk thermolysis studies suggests that the *tert*-butoxy groups in these complexes undergo facile isobutene gas elimination at temperatures often lower than 150 °C.[14−23] In particular, we have been recently successful in synthesizing a variety of monomeric, oligomeric, and polymeric metal−dtbp complexes (Chart 1) which are excellent single-source precursors for metal−phosphate materials.[16−23]

Combining the advantages of both the above-discussed approaches, viz. the use of rigid spacer ligands such as 4,4′-bipyridine ligands in building extended grid structures and

(4) (a) Losier, P.; Zaworotko, M. J. *Angew. Chem., Int. Ed. Engl.* **1996**, *35*, 5, 2779. (b) Fujita, M.; Kwon, Y. J.; Washizu, S.; Ogura, K. *J. Am. Chem. Soc.* **1994**, *116*, 1151. (c) Yaghi, O. M.; Li, H.; Groy, T. L. *Inorg. Chem.* **1997**, *36*, 4292.

(5) (a) Soldatov, D. V.; Tinnemans, P.; Enright, G. D.; Ratcliffe, C. I.; Diamente, P. R.; Ripmeester, J. A. *Chem. Mater.* **2003**, *15*, 3826. (b) Sun, D.; Cao, R.; Sun, Y.; Bi, W.; Li, X.; Wang, Y.; Shi, Q.; Li, X. *Inorg. Chem.* **2003**, *42*, 7512. (c) Rajendran, T.; Manimaran, B.; Liao, R.-T.; Lin, R.-J.; Thanasekaran, P.; Lee, G.-H.; Peng, S.-M.; Liu, Y.-H.; Chang, I.-J.; Rajagopal, S.; Lu, K.-L. *Inorg. Chem.* **2003**, *42*, 6388. (d) Shi, Z.; Li, G.; Wang, L.; Gao, L.; Chen, X.; Hua, J.; Feng, S. *Cryst. Growth Des.* **2004**, *4*, 25. (e) Fu, R.-B.; Wu, X.-T.; Hu, S.-M.; Zhang, J.-J.; Fu, Z.-Y.; Du, W.-X. *Inorg. Chem. Commun.* **2003**, *6*, 827. (f) Yin, P.; Peng, Y.; Zheng, L.-M.; Gao, S.; Xin, X.-Q. *Eur. J. Inorg. Chem.* **2003**, 726. (g) Chang, X.-M.; Chen, X.-M. *Eur. J. Inorg. Chem.* **2003**, 413. (h) Tao, J.; Chen, X.-M.; Huang, R.-B.; Zheng, L.-S. *J. Solid State Chem.* **2003**, *170*, 130. (i) Prior, T. J.; Bradshaw, D.; Teat, S. J.; Rosseinsky, M. J. *Chem. Commun.* **2003**, 500. (j) Cao, R.; Shi, Q.; Sun, D.; Hong, M.; Bi, W.; Zhao, Y. *Inorg. Chem.* **2002**, *41*, 6161.

(6) (a) Liang, Y.-C.; Hong, M.-C.; Cao, R.; Su, W.-P.; Zhao, Y.-J.; Weng, J.-B. *Polyhedron* **2001**, *20*, 2477. (b) Khalid, A. S.; Christoph, J.; Berthold, K. *Acta Crystallogr.* **2001**, C57, 1261. (c) Liao, J.-H.; Chen, P.-L.; Hsu, C.-C. *J. Phys. Chem. Solids* **2001**, *62*, 1629. (d) Tong, M.-L.; Chen, X.-M.; Ng, S. W. *Inorg. Chem. Commun.* **2000**, *3*, 436. (e) Chen, C. Y.; Lo, F. R.; Kao, H. M.; Lii, K. H. *Chem. Commun.* **2000**, 1061. (f) Li, K. H.; Huang, Y. F.; *Inorg. Chem.* **1999**, *38*, 1348. (g) Halasyamani, P.; Drewitt, M. J.; O'Hare, D. *Chem. Commun.* **1997**, 867. (h) Chippindale, A. M.; Turner, C. *J. Solid State Chem.* **1997**, *128*, 318. (i) Zheng, L. M.; Yin, P.; Xin, X. Q. *Inorg. Chem.* **2002**, *41*, 4084.

(7) (a) Shi, Z.; Feng, S.; Zhang, L.; Yang, G.; Hua, J. *Chem. Mater.* **2000**, *12*, 2930. (b) Huang, C. H.; Huang, L. H.; Lii, K. H. *Inorg. Chem.* **2001**, *40*, 2625. (c) Shi, Z.; Feng, S.; Gao, S.; Zhang, L.; Yang, G.; Hua, J. *Angew. Chem., Int. Ed.* **2000**, *39*, 2325. (d) Inman, C.; Knaust, J. M.; Keller, S. W. *Chem. Commun.* **2002**, 156. (e) Glinskaya, L. A.; Shchukin, V. G.; Klevtsova, R. F.; Mazhara, A. P.; Larionov, S. V. *J. Struct. Chem.* **2001**, *41*, 632 (translation of *Zh. Strukt. Khim.* **2000**).

(8) Hoskins B. F.; Robson, R. *J. Am. Chem. Soc.* **1990**, *112*, 1546.

(9) Murugavel, R.; Walawalkar, M. G.; Dan, M.; Roesky, H. W.; Rao, C. N. R. *Acc. Chem. Res.* **2004**, *37*, 763.

(10) Oliver, S.; Kuperman A.; Ozin, G. A. *Angew. Chem., Int. Ed.* **1998**, *37*, 46.

(11) (a) Ayi, A. A.; Choudhury, A.; Natarajan, S.; Neeraj, S.; Rao, C. N. R. *J. Mater. Chem.* **2001**, *11*, 1181. (b) Choudhury, A.; Neeraj, S.; Natarajan, S.; Rao, C. N. R. *J. Mater. Chem.* **2002**, *12*, 1044.

(12) Dan, M.; Udayakumar, D.; Rao, C. N. R. *Chem. Commun.* **2003**, 2212.

(13) (a) Williams, A. G.; Interrante, L. V. In *Better Ceramics Through Chemistry*; Brinker, C. J., Clark, D. E., Ulrich, D. R., Eds.; Materials Research Society Symposia Proceedings; North-Holland Publishers: New York, 1984; Vol 32. (b) Chandler, C. D.; Roger, C.; Hampden-Smith, M. J. *Chem. Rev.* **1993**, *93*, 1205. (c) *Organosilicon Chemistry III: From Molecules to Materials*; Auner, N., Weis, J., Eds.; Wiley-VCH: Weinheim, Germany, 1998.

(14) (a) Lugmair, C. G.; Tilley, T. D.; Rheingold, A. L. *Chem. Mater.* **1997**, *9*, 339. (b) Lugmair, C. G.; Tilley, T. D. *Inorg. Chem.* **1998**, *37*, 1821. (c) Lugmair, C. G.; Tilley, T. D. *Inorg. Chem.* **1998**, *37*, 6304. (d) Lugmair, C. G.; Tilley, T. D.; Rheingold, A. L. *Chem. Mater.* **1999**, *11*, 1615.

(15) Fujdala, K. L.; Oliver, A. G.; Hollander, F. J.; Tilley, T. D. *Inorg. Chem.* **2003**, *42*, 1140 and references therein.

(16) Murugavel, R.; Sathiyendiran, M.; Pothiraja, R.; Walawalkar, M. G.; Mallah, T.; Riviére, E. *Inorg. Chem.* **2004**, *43*, 945.

(17) Sathiyendiran, M.; Murugavel, R. *Inorg. Chem.* **2002**, *41*, 6404.

(18) Murugavel, R.; Sathiyendiran, M.; Walawalkar, M. G. *Inorg. Chem.* **2001**, *40*, 427.

(19) Murugavel, R.; Sathiyendiran, M.; Pothiraja, R.; Butcher, R. J. *Chem. Commun.* **2003**, 2546.

(20) Murugavel, R.; Sathiyendiran, M. *Chem. Lett.* **2001**, 84.

(21) Sathiyendiran, M. Ph.D. Thesis, IIT-Bombay, 2003.

(22) Murugavel, R.; Sathiyendiran, M.; Pothiraja, R.; Walawalkar, M. G.; Mallah, T.; Riviére, E. *Inorg. Chem.* **2004**, *43*, 945.

(23) Pothiraja, R.; Sathiyendiran, M.; Murugavel, R.; Butcher, R. J. *Inorg. Chem.* **2004**, *43*, 7585−7587.

Scheme 1. Synthesis and Conversion of the Metal Phosphates **1**−**11**

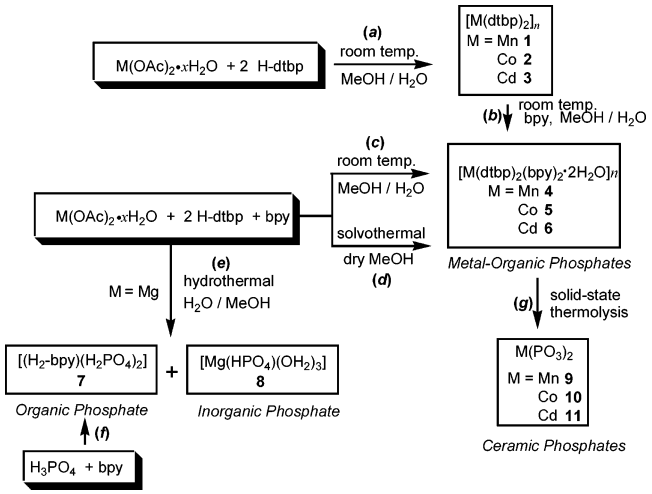

the use of thermally labile ligands such [(^{t}BuO)$_2$P(O)OH] for the synthesis of molecular precursors for ceramic materials, we wish to report herein a new one-dimensional organic soluble metal−phosphate chain that can be readily transformed into a two-dimensional grid structure. A preliminary report of this work has recently appeared.[23]

Results and Discussion

Synthesis. It has been shown from our recent studies that the reaction of metal acetates with [(^{t}BuO)$_2$P(O)(OH)] (dtbp-H) at 25 °C results in the formation of tetrameric phosphates [M$_4$(dtbp)$_6$(μ_4-O)] (M = Zn, Co, Mn).[18] While the addition of strong donor ligands to this reaction breaks these tetramers to monomeric species,[18−20] the use of weak Lewis bases such as THF or DMSO leads to the isolation of one-dimensional polymers.[17] Thus, the reaction of cobalt acetate with dtbp-H in the presence of 3,5-dimethylpyrazole yields the monomeric [Co(dmp)$_2$(dtbp)$_2$];[18] one-dimensional polymers [M(dtbp)$_2$]$_n$ (M = Mn or Co) and [Cd(dtbp)$_2$(OH$_2$)]$_n$ are isolated from the same reaction in the presence of very weak Lewis bases (Scheme 1, path a).[17,23]

After studying the effect of monodentate N-donors such as imidazole and chelating ligands such as 1,10-phenanthroline and 2,2′-bipyridine in the reaction of metal acetate with di-*tert*-butyl phosphate,[18−20] we turned our attention in this study to the rigid ditopic bridging spacer 4,4′-bipyridine. Thus, manganese and cobalt polymers [M(dtbp)$_2$]$_n$ (M = Mn (**1**) or Co (**2**)) transform readily into a two-dimensional grid structures [M(dtbp)$_2$(bpy)$_2$·2H$_2$O]$_n$ (M = Mn (**4**) or Co (**5**)) by stirring **1** or **2** with 2 equiv of bpy in methanol for a few hours, respectively (Scheme 1, path b). This transformation is very general, and the cadmium polymer [Cd(dtbp)$_2$(OH$_2$)]$_n$ (**3**) (made of a 4d metal) is also transformed similarly to [Cd(dtbp)$_2$(bpy)$_2$·2H$_2$O]$_n$ (**6**) under similar conditions in good yields.

Subsequent experiments showed that it is possible to prepare the 2-D grid structures **4**−**6** in one-step, without going through the 1-D molecular wires **1**−**3**, by a direct reaction between the metal acetate, di-*tert*-butyl phosphate (dtbp-H), and 4,4′-bipyridine (bpy) in a 1:2:2 molar ratio in methanol (or ethanol)/water mixture, in good yields (Scheme 1, path c). Irrespective of the methodology used, in all the cases the final products could be obtained as pure single crystals on repeated crystallization from methanol. The recrystallized samples were found to be insoluble in solvents such as benzene, toluene, and petroleum ether.[24]

To study the effect of autogenous pressure and elevated reaction temperature in the formation of two-dimensional grid structures, the above reactions were carried out in dry methanol in a sealed Pyrex tube at 75−80 °C for 30 h. On the basis of earlier results on solid-state thermolysis of di-*tert*-butyl phosphate complexes,[17,18] it was expected that the solvothermal reactions will produce two-dimensional grid structures of the type [M(H$_2$PO$_4$)$_2$(bpy)$_2$·2H$_2$O]$_n$, where the ^{t}BuO groups of the dtbp ligand would undergo a β-H elimination liberating isobutene and leaving a OH group on phosphorus. However, such a β-H elimination reaction did not take place in the present case and only the two-dimensional structures **4**−**6** were isolated as the products in all solvothermal reactions (Scheme 1, path d).

When the above reaction was repeated to prepare the magnesium analogue [Mg(dtbp)$_2$(bpy)$_2$·2H$_2$O]$_n$, either by room-temperature mixing or by the solvothermal method, only a complex mixture of products was obtained and no pure compound could be crystallized from this product mixture. Hence the synthesis of [Mg(dtbp)$_2$(bpy)$_2$·2H$_2$O]$_n$ was attempted under *hydrothermal conditions* (Scheme 1, path e). At the beginning of the hydrothermal reaction the reaction mixture was heterogeneous due to the insolubility of metal acetate in methanol. The use of water along with methanol under hydrothermal conditions, however, results in a clear reaction mixture before the start of the reaction. As the reaction proceeds, a microcrystalline product, later analyzed as [Mg(HPO$_4$)(OH$_2$)$_3$] (**8**), formed at the bottom of the sealed tube. Filtration of this product at the end of the reaction and leaving the filtrate for crystallization afforded a second product, which was found to be [(H$_2$bpy)(H$_2$PO$_4$)$_2$] (**7**). While the inorganic magnesium hydrogen phosphate trihydrate **8** has been known for a long time and is synthesized using a variety of routes, the synthesis of organic phosphate **7** is achieved for the first time. To probe the role of magnesium acetate Mg(OAc)$_2$ during the synthesis, H$_3$PO$_4$ was directly reacted with bpy in methanol (Scheme 1, path f). Compound **7** was obtained as the major crystalline product on slow evaporation of the solvent from the reaction mixture.

Spectra. Compounds **4**−**7** have been characterized using elemental analysis, IR and UV−vis spectroscopy, thermal analysis, and single-crystal X-ray diffraction studies. Selected analytical and spectroscopic data are listed in Table 1. The bands observed around 3460 cm^{-1} in the IR spectra suggest the presence of coordinated or lattice water molecules in compounds **4**−**6**. The strong absorptions observed at 1196,

(24) It is possible that compounds **4**−**6** exist as molecular species in methanol but, on crystallization, they assemble into the 2-D grid structures that are insoluble in other common organic solvents. The solution IR spectra of **4**−**6** in methanol show significant differences compared to the spectra recorded in the solid state as KBr pellets indicating the possible presence of molecular species in solution.

Table 1. Selected Analytical and Spectroscopic Data

compd	yield, %	elemental anal., %: found (calcd) C	H	N	ν(P═O)/ν(P−O−M), cm^{-1}	^{31}P NMR δ, ppm
4	63	52.7 (52.6)	6.9 (6.9)	6.9 (6.8)	1196, 1081, 976	
5	79	52.1 (52.4)	6.5 (6.8)	7.2 (6.8)	1197, 1085, 974	
6	66	49.3 (49.2)	6.6 (6.4)	6.5 (6.4)	1187, 1076, 976	4.77
7	97	34.2 (34.1)	3.4 (3.5)	7.8 (8.0)	1119, 978	0.37

1081, and 976 cm^{-1} for **4**, 1197, 1085, and 974 cm^{-1} for **5**, and 1187, 1076, and 976 cm^{-1} for **6** are due to the phosphoryl group (P═O)/M−O−P linkages.[25] The large shift observed in the case of phosphoryl group absorption compared to the free dtbp-H might be due attributed to the presence of hydrogen bonds between the phosphoryl oxygen atoms and the water molecules. The UV−vis spectra of **4**−**6** in methanol solution show an absorption maximum at around 290 nm (296 nm for **4**, 291 nm for **5**, and 298 nm for **6**) which may be assigned to the absorption due to the $\pi \rightarrow \pi^*$ absorption of the 4,4′-bipyridyl group.

In the ^{1}H NMR spectrum of **6**, the protons of the *tert*-butyl groups resonate as a singlet at δ 1.42 ppm while an AA′BB′ spectral pattern is observed for the protons of the bipyridine ligand with resonances appearing at δ 7.85 and 8.71 ppm, respectively. In the ^{31}P NMR spectrum, a single resonance was observed at δ 4.77 ppm, indicating the presence of only one type of dtbp ligand in compound **6**. This resonance is shifted ca. 1.3 ppm downfield from the free ligand. The ^{31}P NMR spectrum of the organic phosphate **7** shows a single resonance at δ 0.37 ppm, which is only very slightly shifted from the value for H_3PO_4.

Molecular Structures of 2 and 4−6. The details of the crystal structure of one-dimensional polymer **2** have been described in detail in the preliminary communication.[23] Storing a methanol solution containing manganese acetate, dtbp-H, and 4,4′-bipyridine at ~25 °C over 4 days gave pale yellow X-ray-quality single crystals of **4**. Compounds **5** and **6** were also crystallized in a similar fashion. Compounds **4** and **5** crystallize in monoclinic *P*2/*c* space group and are isomorphous. Selected structural parameters observed for compounds **4**−**6** are listed in Tables 2−4, respectively.

There are two crystallographically unique manganese ions (each 0.5 occupancy) in the asymmetric part of **4**. Manganese ions in this extended solid have octahedral coordination geometry and are connected to four 4,4′-bipyridine moieties and two dtbp ligands in a trans arrangement (Figure 1). Each of the 4,4′-bipyridine ligand bridges two manganese atoms in an end-to-end fashion. The two unique manganese ions present in the system make two separate two-dimensional grids, and one such grid is shown in Figure 2. These two unique grids lie one over the other in such as way that the metal ion on the second grid is in the middle of the cavity of the first grid to minimize the steric repulsion between the bulky phosphate ligands on the adjacent grids.

In the grid formed by Mn(1), there are two unique 4,4′-bipyridine ligands. These ligands differ from each other by the twist between the two pyridyl rings of the bipyridine (0 and 30°, respectively). Similarly, the twist angles between the pyridyl rings of bipyridine in the second grid are 0 and 9°, respectively. These observed twists are largely responsible for the wavelike propagation of the polymer in any given axis. The Mn−O bond distance is slightly shorter in Mn(2) (2.097(2) Å) than in Mn(1) (2.124(2) Å). These values are similar to those observed in the case of the one-dimensional polymer [Mn(dtbp)$_2$].[17] The observed Mn−N bond lengths are consistent with similar distances found for related Mn−pyridyl complexes.[26] The observed Mn···Mn distances, which offer an estimate of the size of the rectangular windows present in these systems, in the grid structure of **4** are shown in Figure 3. Interestingly, along the chain of

Table 2. Selected Bond Lengths (Å) and Angles (deg) for [Mn(dtbp)$_2$(bpy)$_2$·2H$_2$O]$_n$ (**4**)[a]

Mn(1)−O(1)	2.124(2)	Mn(2)−O(5)	2.097(2)
Mn(1)−N(2)	2.296(2)	Mn(2)−N(4)	2.312(3)
Mn(1)−N(1)	2.322(2)	Mn(2)−N(5)[c]	2.273(3)
Mn(2)−N(3)[d]	2.360(2)		
O(1)[a]−Mn(1)−O(1)	180.0	O(5)−Mn(2)−O(5)[b]	179.9(1)
N(2)[a]−Mn(1)−N(2)	180.0	N(5)[c]−Mn(2)−N(4)	180.0
N(1)[a]−Mn(1)−N(1)	180.0	N(3)[d]−Mn(2)−N(3)[e]	173.1(1)
N(2)[a]−Mn(1)−N(1)[a]	88.42(7)	N(4)−Mn(2)−N(3)[e]	86.55(5)
N(2)−Mn(1)−N(1)[a]	91.58(7)	N(5)[c]−Mn(2)−N(3)[e]	93.45(5)
O(1)[a]−Mn(1)−N(2)[a]	90.02(8)	O(5)−Mn(2)−N(5)[c]	89.94(5)
O(1)−Mn(1)−N(2)[a]	89.98(8)	O(5)−Mn(2)−N(4)	90.06(5)
O(1)−Mn(1)−N(1)[a]	90.29(7)	O(5)−Mn(2)−N(3)[d]	90.56(7)
O(1)−Mn(1)−N(1)	89.71(7)	O(5)−Mn(2)−N(3)[e]	89.45(7)

[a] Symmetry transformations: (a) $-x+2, -y, -z+2$; (b) $-x+3, y, -z+3/2$; (c) $x, y-1, z$; (d) $-x+3, -y-1, -z+2$; (e) $x, -y-1, z-1/2$.

Table 3. Selected Bond Lengths (Å) and Angles (deg) for [Co(dtbp)$_2$(bpy)$_2$·2H$_2$O]$_n$ (**5**)[a]

Co(1)−O(1)	2.067(5)	Co(1)−N(1)	2.196(5)
Co(1)−N(2)	2.180(5)	Co(2)−O(5)	2.044(6)
Co(2)−N(3)	2.250(6)	Co(2)−N(4)	2.092(9)
Co(2)−N(5)	2.141(9)	P(1)−O(1)	1.486(5)
P(1)−O(2)	1.599(5)	P(1)−O(3)	1.559(6)
P(1)−O(4)	1.484(5)	P(2)−O(5)	1.505(6)
P(2)−O(6)	1.585(5)	P(2)−O(7)	1.607(5)
P(2)−O(8)	1.466(6)		
O(1)[a]−Co(1)−O(1)	180.0	N(1)[a]−Co(1)−N(1)	180.0
N(2)[a]−Co(1)−N(2)	180.0	O(1)−Co(1)−N(1)	90.9(2)
N(2)−Co(1)−N(1)	88.3(2)	O(1)−Co(1)−N(2)	90.0(2)
O(5)[b]−Co(2)−O(5)	178.0(3)	N(4)−Co(2)−N(5)	180.0
N(3)[b]−Co(2)−N(3)	174.5(3)	O(5)−Co(2)−N(5)	91.0(2)
O(5)−Co(2)−N(3)	90.5(2)	N(4)−Co(2)−N(3)	87.3(2)
N(5)−Co(2)−N(3)	92.7(2)	O(5)−Co(2)−N(4)	89.0(2)
O(4)−P(1)−O(1)	117.2(3)	O(4)−P(1)−O(2)	110.6(3)
O(4)−P(1)−O(3)	112.5(3)	O(3)−P(1)−O(2)	103.8(3)
O(1)−P(1)−O(3)	102.8(3)	O(1)−P(1)−O(2)	108.9(3)
O(8)−P(2)−O(7)	114.1(3)	O(8)−P(2)−O(6)	113.2(3)
O(8)−P(2)−O(5)	116.6(3)	O(6)−P(2)−O(7)	99.7(3)
O(5)−P(2)−O(7)	102.0(3)	O(5)−P(2)−O(6)	109.4(3)

[a] Symmetry transformations used to generate equivalent atoms: (a) $-x, -y, -z$; (b) $-x+1, y, -z+3/2$.

(25) (a) Thomas, L. C. *Interpretation of the Infrared Spectra of Organophosphorus Compounds*; Heyden and Son: Chichester, U.K., 1974. (b) Bellamy, L. J. *The Infrared Spectra of Complex Molecules*; Chapman and Hall: London, 1975.

Table 4. Selected Bond Lengths (Å) and Angles (deg) for $[Cd(dtbp)_2(bpy)_2 \cdot 2H_2O]_n$ (**6**)[a]

Cd(1A)−O(1A)	2.220(3)	Cd(1B)−O(1B)	2.283(3)
Cd(1A)−N(3A)	2.331(4)	Cd(1B)−N(11D)	2.343(3)
Cd(1A)−N(1A)	2.379(4)	Cd(1B)−N(11A)	2.361(3)
Cd(1A)−N(2A)	2.404(3)	Cd(1B)−N(11B)	2.362(3)
Cd(1B)−O(11B)	2.260(3)	Cd(1B)−N(11C)	2.365(3)
O(1A)[a]−Cd(1A)−O(1A)	179.6 (2)	O(11B)−Cd(1B)−O(1B)	178.0(1)
N(3A)−Cd(1A)−N(1A)	180.0	N(11D)−Cd(1B)−N(11B)	179.0(1)
N(2A)−Cd(1A)−N(2A)[a]	170. 9(2)	N(11A)−Cd(1B)−N(11C)	176.2(1)
O(1A)−Cd(1A)−N(3A)	90.22(8)	O(1B)−Cd(1B)−N(11A)	89.3(1)
O(1A)−Cd(1A)−N(2A)[a]	91.6(1)	N(11D)−Cd(1B)−N(11A)	89.7(1)
O(1A)−Cd(1A)−N(1A)	89.78(8)	O(1B)−Cd(1B)−N(11B)	93.1(1)
O(1A)−Cd(1A)−N(2A)	88.4(1)	O(11B)−Cd(1B)−N(11B)	88.8(1)
N(3A)−Cd(1A)−N(2A)	94.56(7)	N(11A)−Cd(1B)−N(11B)	89.8(1)
N(1A)−Cd(1A)−N(2A)	85.44(7)	O(11B)−Cd(1B)−N(11D)	90.3(1)
N(11B)−Cd(1B)−N(11C)	86.7(1)	O(1B)−Cd(1B)−N(11D)	87.8(1)
O(11B)−Cd(1B)−N(11A)	90.2(1)	O(11B)−Cd(1B)−N(11C)	88.2(1)
O(1B)−Cd(1B)−N(11C)	92.4(1)	N(11D)−Cd(1B)−N(11C)	93.8(1)

[a] Symmetry transformations: (a) $-x, y, 3/2 - z$.

propagation, the distances are approximately 11.7−11.9 Å, while the distances across the grid window are 15.5 and 17.8 Å, indicating the grid windows are not exactly rectangular but parallelepipeds. The sum of the angles within any given parallelepiped is 360° (Figure 3). The size of this voids, hence, allows incorporation of two water molecules/formula unit of the metal. These water molecules are hydrogen bonded to the phosphoryl oxygens of the phosphate group.

Although $[Cd(dtbp)_2(bpy)_2 \cdot 2H_2O]_n$ (**6**) crystallizes in a different monoclinic space group (*C*2/*c*), its molecular structure is very similar to the manganese and cobalt compounds **4** and **5**. In the asymmetric part of **6**, as in the case of **4** and **5**, two crystallographically unique Cd^{2+} ions are present. While one of the cadmium ions has a full occupancy, the other cadmium ion has an occupancy of 0.5. Both the unique cadmium ions form two independent grid structures with the help of bpy ligands as in the case of **4** and **5**. A section of the two adjacent grids shown in Figure 4 clearly reveals that the cavities formed by one rectangular grid are partially filled by the organic substituents from the adjacent grid. A view perpendicular to the plane of this grid (Figure 4b) shows the highly planar nature of the grid as well as the perfect axial disposition of the dtbp ligands at the metal centers. The observed Cd−O(phosphate) distances in **6** are marginally longer than those observed in the case of the one-dimensional polymer $[Cd(dtbp)_2(OH_2)]$, where the dtbp functions as a bidentate bridging ligand.[17] The observed

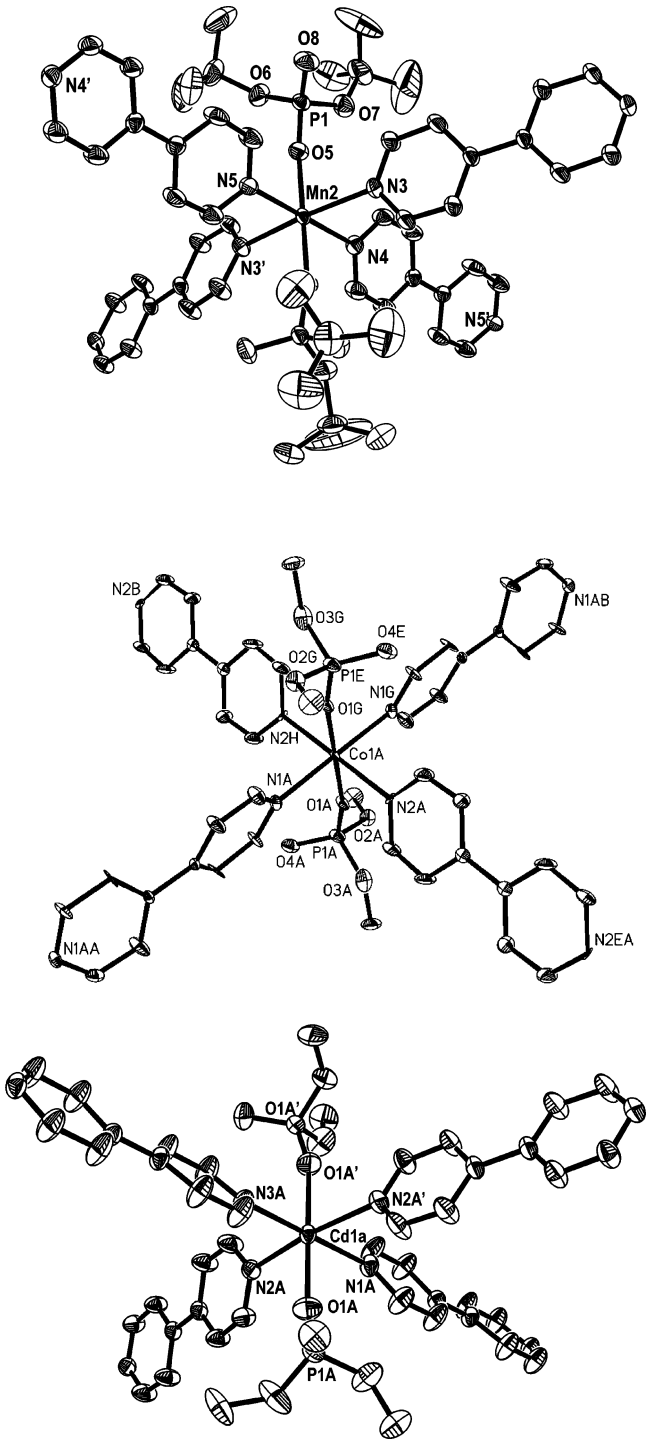

Figure 1. ORTEP (50% probability level) showing the local coordination geometries around one of the crystallographically unique Mn, Co, and Cd ions in **4**−**6**. In all the cases the methyl groups of the *tert*-butyl substituent are omitted for clarity.

Cd−N distances in the structure of **6** are comparable to the similar distances of cadmium−bipyridyl complexes described in the literature.[27] The dimensions of the cavity created in the cadmium structure are schematically represented in Figure 3. It is interesting to note that the dimensions of the cavity in **6** are very similar to those of the cavity observed in the case of **4** and **5**, is spite of the fact that cadmium is a 4d metal. However, the observed comparable M−N distances in **4**−**6** in the two structures explain this observation.

(26) (a) Koo, B.-K.; Bewley, L.; Golub, V.; Rarig, Randy S.; Burkholder, E.; O'Connor, C. J.; Zubieta, J. *Inorg. Chim. Acta* **2003**, *351*, 167. (b) Dong, W.; Wang, Q.-L.; Si, S.-F.; Liao, D.-Z.; Jiang, Z.-H.; Yan, S.-P.; Cheng, P. *Inorg. Chem. Commun.* **2003**, *6*, 873. (c) Rodriguez-Martin, Y.; Hernandez-Molina, M.; Sanchiz, J.; Ruiz-Perez, C.; Lloret, F.; Julve, M. *J. Chem. Soc., Dalton Trans.* **2003**, 2359. (d) Ma, C.; Chen, C.; Liu, Q.; Liao, D.; Li, L.; Sun, L. *New J. Chem.* **2003**, *27*, 890. (e) Nedelcu, A.; Zak, Z.; Madalan, A. M.; Pinkas, J.; Andruh, M. *Polyhedron* **2003**, *22*, 789. (f) Maji, T. K.; Sain, S.; Mostafa, G.; Lu, T.-H.; Ribas, J.; Monfort, M.; Chaudhuri, N. R. *Inorg. Chem.* **2003**, *42*, 709. (g) Escuer, A.; Sanz, N.; Vicente, R.; Mautner, F. A. *Inorg. Chem.* **2003**, *42*, 541. (h) Darriet, J.; Massa, W.; Pebler, J.; Stief, R. *Solid State Sci.* **2002**, *4*, 1499. (i) Wang, Y.; Feng, L.; Li, Y.; Hu, C.; Wang, E.; Hu, N.; Jia, H. *Inorg. Chem.* **2002**, *41*, 6351. (j) Oh, M.; Carpenter, G. B.; Sweigart, D. A. *Angew. Chem., Int. Ed.* **2002**, *41*, 3650. (k) Naether, C.; Greve, J.; Je, I. *Chem. Mater.* **2002**, *14*, 4536. (l) Jensen, P.; Batten, S. R.; Moubaraki, B.; Murray, K. S. *J. Chem. Soc., Dalton Trans.* **2002**, 3712.

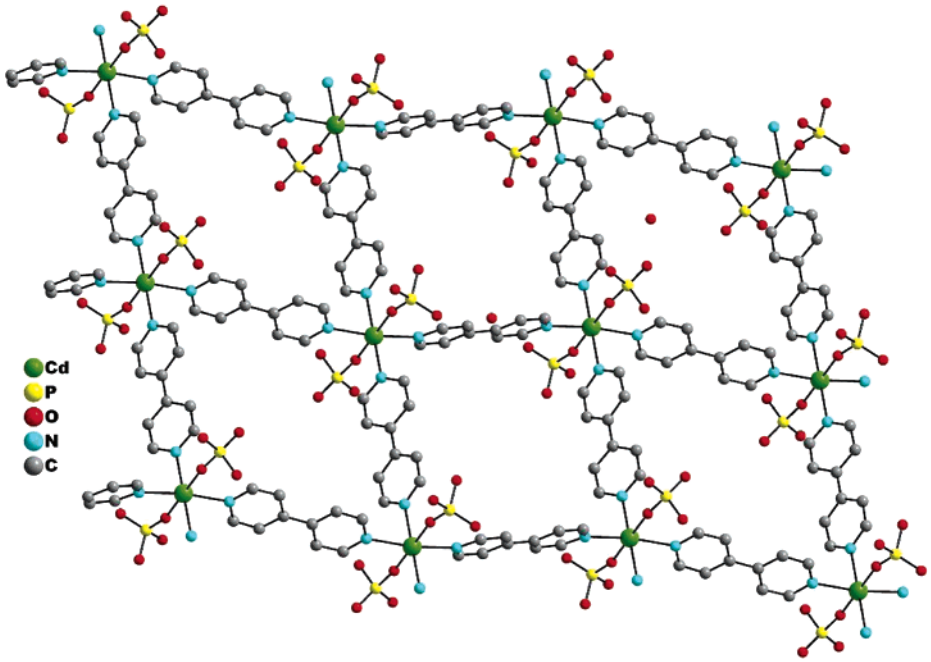

Figure 2. Ball and stick model of the two-dimensional grid structure formed in the crystal structure of $[Mn(dtbp)_2(bpy)_2 \cdot 2H_2O]_n$ (**4**) (view down *a*). The grid formed by the cobalt and cadmium compounds **5** and **6** also have very similar structures. The *tert*-butyl groups are omitted for clarity.

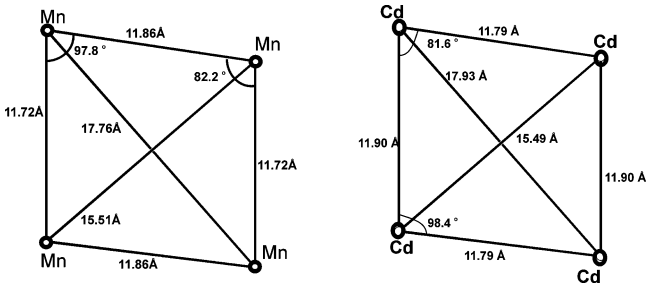

Figure 3. Dimensions of the rectangular windows in the molecular structure of $[Mn(dtbp)_2(bpy)_2 \cdot 2H_2O]_n$ (**4**) and $[Cd(dtbp)_2(bpy)_2 \cdot 2H_2O]_n$ (**6**).

Structure of Layered Organic Phosphate 7. Crystals of organic phosphate **7** suitable for diffraction studies were directly obtained from the hydrothermal reaction as described above (Scheme 1, path e). The structure of the organic phosphate **7** is very interesting in the light of enormous interest in the area of amine−phosphates in recent years as starting materials for new framework metal phosphate structures.[28] Compound **7** crystallizes in the centerosymmetric space group $P2_1/c$. The contents of the repeating unit are shown in Figure 5. The arrangement of the $[H_2bpy]^{2+}$ cations and $[H_2PO_4]^-$ anions in the lattice of **7**, viewed down the *a* axis, is shown in Figure 6. Through O−H···O, N−H···O, and aromatic C−H···O interactions, the cations and anions form an extended two-dimensional structure (Table 5). These two-dimensional sheets are further linked to each other through additional hydrogen-bonding interactions to form the final three-dimensional structure. The extended three-dimensional structure of compound **7** is best described as a layered lattice where organic $[H_2bpy]^{2+}$ and inorganic $[H_2PO_4]^-$ layers alternate periodically throughout the crystal. Thus, it can be inferred from its physical properties and molecular structure that compound **7** could be a useful organic soluble source of dihydrogen phosphate $[H_2PO_4]^-$ anion for the preparation of other metal phosphates starting from metal halides.

Thermolysis Studies. The presence of *tert*-butoxy groups makes compounds **4**−**6** ideal candidates for solid-state decomposition to produce phosphate materials. The presence of a fairly rigid coligand present in the complex, viz. bipyridine, suggested that it may be possible to convert the M−dtbp groups in **4**−**6** into $M-H_2PO_4$ groups without the grid structure collapsing. In such a case, it would be

(27) (a) Dai, J.-C.; Hu, S.-M.; Wu, X.-T.; Fu, Z.-Y.; Du, W.-X.; Zhang, H.-H.; Sun, R.-Q. *New J. Chem.* **2003**, *27*, 914. (b) Xu, Y.; Bi, W.-H.; Li, X.; Sun, D.-F.; Cao, R.; Hong, M.-C. *Inorg. Chem. Commun.* **2003**, *6*, 495. (c) Tao, J.; Chen, X.-M.; Huang, R.-B.; Zheng, L.-S. *J. Solid State Chem.* **2003**, *170*, 130. (d) Davidson, G. J. E.; Loeb, S. J. *Angew. Chem., Int. Ed.* **2003**, *42*, 74. (e) Li, L.; Chen, B.; Song, Y.; Li, G.; Hou, H.; Fan, Y.; Mi, L. *Inorg. Chim. Acta* **2003**, *344*, 95. (f) Vittal, J. J.; Sampanthar, J. T.; Lu, Z. *Inorg. Chim. Acta* **2003**, *343*, 224. (g) Almeida Paz, F. A.; Bond, A. D.; Khimyak, Y. Z.; Klinowski, J. *Acta Crystallogr.* **2002**, *C58*, m608. (h) Selby, H. D.; Orto, P.; Carducci, M. D.; Zheng, Z. *Inorg. Chem.* **2002**, *41*, 6175. (i) Yoshikawa, H.; Nishikiori, S.-I.; Watanabe, T.; Ishida, T.; Watanabe, G.; Murakami, M.; Suwinska, K.; Luboradzki, R.; Lipkowski, J. *J. Chem. Soc., Dalton Trans.* **2002**, 1907.

(28) Amine−phosphates: (a) Neeraj, S.; Natarajan, S.; Rao, C. N. R. *Angew. Chem., Int. Ed.* **1999**, *38*, 3480. (b) Sharma, C. V. K.; Clearfield, A. *J. Am. Chem. Soc.* **2000**, *122*, 4394. (c) Mahmoudkhani, A. H.; Langer, V. *Acta Crystallogr.* **2001**, *E57*, i19. (d) Mahmoudkhani, A. H.; Langer, V. *Acta Crystallogr.* **2001**, *E57*, o866. (e) Mahmoudkhani, A. H.; Langer, V. *J. Mol. Struct.* **2002**, *609*, 55. (f) Mahmoudkhani, A. H.; Langer, V. *J. Mol. Struct.* **2002**, *609*, 97. (g) Ferguson, G.; Glidewell, C.; Gregson, R. M.; Meehan, P. R. *Acta Crystallogr.* **1998**, *B54*, 129. (h) Gregson, R. M.; Glidewell, C.; Ferguson, G.; Lough, A. J. *Acta Crystallogr.* **2000**, *B56*, 39. (i) Wheatley, P. S.; Lough, A. J.; Ferguson, G.; Burchell, C. J.; Glidewell, C. *Acta Crystallogr.* **2001**, *B57*, 95. (j) Glidewell, C.; Ferguson, G.; Lough, A. J. *Acta Crystallogr.* **2000**, *C56*, 855. (k) Fuller, J.; Heimer, N. E. *J. Chem. Crystallogr.* **1995**, *25*, 129. (l) Mahmoudkhani, A. H.; Langer, V. *Solid State Sci.* **2001**, *3*, 519. (m) Sharma, C. V. K.; Hessheimer, A. J.; Clearfield, A. *Polyhedron* **2001**, *20*, 2095. (n) Cao, G.; Lynch, V. M.; Swinnea, J. S.; Mallouk, T. E. *Inorg. Chem.* **1990**, *29*, 2112. (o) Paixão, J. A.; Matos B. A.; Silva, M. R.; Martin-Gil, J. *Acta Crystallogr.* **2000**, *C56*, 1132.

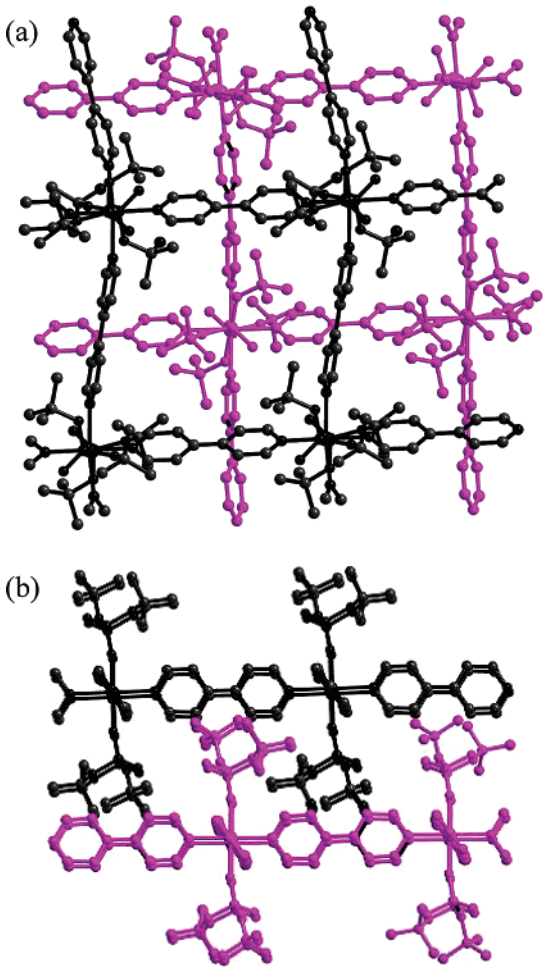

Figure 4. Ball and stick diagram of sections of two contiguous 2-D grids (pink and black) in the lattice showing the partial filling of the internal voids by bulky axial dtbp ligands: (a) view down "*a*"; (b) view down "*b*". Hydrogen atoms are omitted for clarity.

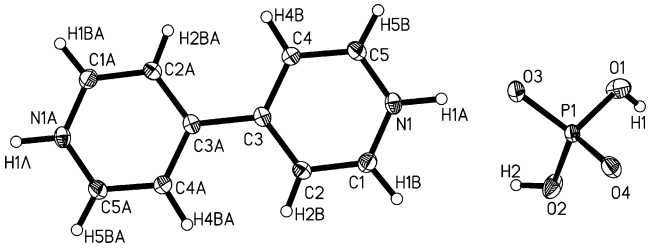

Figure 5. ORTEP diagram of the repeating unit of $[(4,4'\text{-bpyH}_2)^{2+}(H_2PO_4)_2]_n$ (**7**).

necessary to obtain information regarding the exact temperature range at which the P−O−^{t}Bu group converts into P−OH groups through the elimination of isobutene. Thus, to study the feasibility of using **4**−**6** as precursors for the preparation of other phosphates, the thermogravimetric analysis has been performed in an atmosphere of dinitrogen in the temperature range 25−700 °C. The results obtained are listed in Table 6. The TGA−DTA trace for **6** is shown as a representative case in Figure 7. As listed in Table 6, all the grid phosphates synthesized in this study show a very similar thermal decomposition behavior. The three weight losses observed in the range <100, 100−300, and >300 °C correspond to the successive loss of (a) lattice water, (b) isobutene and 4,4′-bipyridine (almost simultaneously), and (c) water due to P−OH condensation.

In the TGA trace for $[Mn(dtbp)_2(bpy)_2\cdot 2H_2O]_n$ (**4**), the first weight loss (4.4%) observed between 60 and 110 °C corresponds to the loss of two uncoordinated water molecules/formula unit. Corresponding to the above weight loss an endotherm was observed at 107 °C in the DSC. The second major weight loss occurs in the range 110−300 °C due to the loss of four isobutene molecules and two 4,4′-bipyridine molecules. The DSC curve also shows a strong endotherm at 208 °C for this weight loss. The final weight loss, which extends up to 700 °C, corresponds to the loss of two water molecules due to a P−OH condensation reaction. The TGA of **5** under N_2 reveals a weight loss of 47% in the range 114−152 °C corresponding to the loss of 4 equiv of isobutene to produce $[Co(O_2P(OH)_2)]$. Heating the sample up to 350 °C results in a further weight loss that corresponds to the removal of two water molecules to result in $Co(PO_3)_2$. $[Cd(dtbp)_2(bpy)_2\cdot 2H_2O]_n$ (**6**) shows a thermogravimetric pattern similar to that of **4** (Figure 7). The first weight loss occurs between 60 and 110 °C (loss of lattice water) while all organic groups are lost (61%) between 120 and 350 °C. The final weight loss (4.1%) corresponding to the condensation of P−OH groups extends up to 700 °C.

The residual mass present in the crucible, after the TGA decomposition up to 700 °C, corresponds to the formation of the metaphosphate material in each case (Table 6). The production of metaphosphate materials in these cases has also been independently verified by carrying out bulk thermolysis of the samples **4**−**6** using the decomposition temperatures inferred from TGA. Typically, the 1 g of each sample was independently pyrolyzed in air at 600 °C for a few hours in a temperature-controlled furnace. As expected, the pyrolysis of **4**−**6** produced $Mn(PO_3)_2$, $Co(PO_3)_2$, and $Cd(PO_3)_2$ materials, respectively (Scheme 1, path g). The products were identified readily by their diffraction pattern matching with those of the authentic samples.[29−31] When the bulk decomposition of **4**−**6** was continued beyond 600 °C, the formation of small quantities of the pyrophosphate $M_2P_2O_7$ along with $M(PO_3)_2$ was observed as revealed by the powder diffraction pattern of the product and its comparison with those of the authentic samples prepared independently. The formation of pyrophosphate is not surprising in view of our recent observation that prolonged heating of copper metaphosphate leads to the release of P_2O_5 and formation of $Cu_2P_2O_7$.[22] Thus, compounds **4**−**6** are good precursors for metaphosphate materials, which however slowly transform into the corresponding pyrophosphate material on prolonged heating.

(29) $Mn(PO_3)_2$: (a) Bukhalova, G. A.; Rabkina, I. G.; Mardirosova, I. V. *Russ. J. Inorg. Chem. (Engl. Transl.)*, **1975**, *20*, 332. (b) *Powder Diffraction File*; International Center for Diffraction Data: Newtowne Square, PA, 1995; Card-36-0210.
(30) $Co(PO_3)_2$: *Powder Diffraction File*; International Center for Diffraction Data: Newtowne Square, PA, 1995; Card-28-0708.
(31) (a) $Cd(PO_3)_2$: *Powder Diffraction File*; International Center for Diffraction Data: Newtowne Square, PA, 1995; Card-39-0165. (b) $Cd_2P_2O_7$: *Powder Diffraction File*; International Center for Diffraction Data: Newtowne Square, PA, 1995; Card-31-0233.

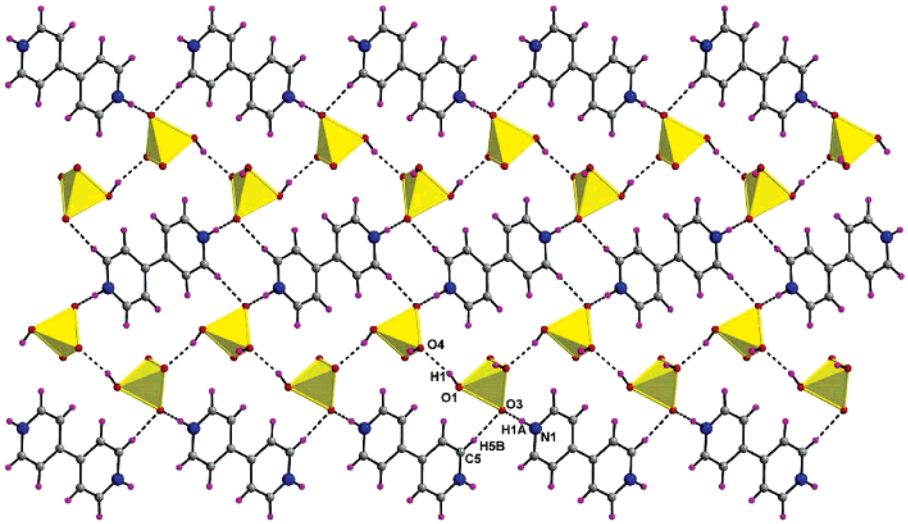

Figure 6. Packing diagram for **7**. (The yellow tetrahedron denotes the PO_4 unit.)

Table 5. Intra- and Intermolecular Hydrogen Bond Distances and Angles in **7**

H-bonds	D−H, Å	D···A, Å	H···A, Å	−D−H···A, deg
N(1)−H(1)···O3	1.00(2)	2.552(2)	1.55(2)	179(2)
O(2)−H(2)···O(4)	0.82(3)	2.519(2)	1.73(3)	164(3)
C(5)−H(5)···O(3)	0.95(2)	3.348(2)	2.40(2)	172(2)
O(1)−H(1)···O(4)	0.77(3)	2.586(2)	1.83(3)	165(3)

Conclusion

This study reveals that the synthesis of non-interpenetrating polymeric grid structures can be achieved by the use of a sterically more demanding dialkyl phosphate on the axial position of octahedral metal centers, whereas in previous investigations the use of noncoordinating anions (such as ClO_4^- or PF_6^-) or smaller anionic ligands (e.g. halides) for building rectangular two-dimensional grid structures often leads to the isolation of either an interpenetrated network or anion enclathrated structures.[3−6]

We have further shown that a new 1-dimensional structural form of cobalt phosphate, $Co(dtbp)_2$, can be converted in to a two-dimensional grid structure in a facile manner by room-temperature reactions. An alternative synthetic route for the synthesis of the grid structures, bypassing the 1-D polymers, has also been developed. Attempted solvothermal variations also result in the formation of the same grid structures with the *tert*-butyl groups intact, while the application of hydrothermal routes resulted in the isolation of a new organic phosphate with layered structure. Finally, molecular grid structures have been recently implicated as useful materials for several applications. In this context, compounds **4**−**6** with thermally labile *tert*-butyl groups on the axial ligands of the metal ions offer new possibilities. We are presently exploring these aspects.

Experimental Section

Instruments and Methods. All the starting materials and the products were found to be stable toward moisture and air, and no specific precautions were taken to rigorously exclude air. Elemental analyses were performed on a Carlo Erba (Milan, Italy) model 1106 elemental analyzer at IIT-Bombay. Infrared spectra were performed on a Nicolet Impact 400 or Nicolet AVTAR 320 spectrometer as KBr-diluted disks. UV−visible spectral studies were carried out on a Shimadzu UV-260 spectrophotometer at room temperature. Powder XRD measurements were obtained on a Philips PW1729 X-ray powder diffractometer. The thermal analysis has been carried out in N_2 (flow rate: 10 mL/min) with the heating rate of 10 °C min^{-1} on a Perkin-Elmer Pyris thermal analyzer.

Solvents and Starting Materials. Commercial grade solvents were purified by employing conventional procedures and were distilled prior to their use.[32] Commercially available starting materials such as $Mn(OAc)_2{\cdot}4H_2O$ (E. Merck), $Cd(OAc)_2{\cdot}2H_2O$ (Aldrich), and 4,4′-bipyridine (Lancaster) were used as received. Di-*tert*-butyl phosphate (dtbp-H) was synthesized from di-*tert*-butyl phosphite using a previously reported procedure.[33] Owing to its thermal instability, dtbp-H was freshly prepared from its potassium salt each time prior to its use. Synthesis of **1** and **3** have been carried out as described earlier.[17]

Synthesis of $[Co(dtbp)_2]_n$ (2). To $[Co(OAc)_2{\cdot}4H_2O]$ (249 mg, 1 mmol) in methanol (30 mL) were added solid dtbp-H (420 mg, 2 mmol) and bis(3,5-dimethylpyrazole)-2-propanol (248 mg, 1 mmol), and the solution was filtered. The filtrate left for crystallization produced X-ray-quality crystals of **2**. Yield: 73%. Anal. Calcd for $C_{16}H_{36}CoO_8P_2$: C, 40.3; H, 7.6. Found: C, 40.0; H, 7.6. IR (KBr, cm^{-1}): 2980 (s), 2934 (m), 1486 (m), 1385 (m), 1370 (m), 1252 (m), 1178 (s), 1090 (s), 1076 (vs), 1038 (s), 992 (vs), 916 (m), 841 (m), 709 (m). TGA [temp range, °C (% weight loss)]: 114−152 (47.2); 152−328(6.4). DSC (°C): 130 (endo); 679 (exo).

Conversion of 1 to 4. Polymer $[Mn(dtbp)_2]$ (1 mmol) was dissolved in methanol (40 mL), and solid bipy (2 mmol) was added and stirred for a few hours. The resulting solution was filtered and kept at room temperature to yield **4** as single crystals in 63% yield.

Alternate Route for Synthesis of 4. Solid dtbp-H (420 mg, 2 mmol) was dissolved in methanol (5 mL), and the solution was added to a methanolic solution (50 mL) of $Mn(OAc)_2{\cdot}4H_2O$ (244 mg, 1 mmol) under constant stirring. Solid 4,4′-bipyridine (312 mg, 2 mmol) was added to the above mixture, and the resultant solution was allowed to stand for 7 d. Yellow crystals of **4** were obtained from the resultant yellow solution. Recrystallization of the sample

(32) Perrin, D. D.; Armarego, W. L. F. *Purification of Laboratory Chemicals*, 3rd ed.; Pergamon Press: London, 1988.
(33) Zwierzak, A.; Kluba, M. *Tetrahedron* **1971**, *27*, 3163.

Table 6. Summary of the Thermal Analysis (TGA) for $[M(dtbp)_2(bpy)_2 \cdot 2H_2O]_n$

molecular formula	thermolysis temp range, °C			tot. wt loss (%):[d] found (calcd)	final mater obtaind
	$-H_2O$[a]	−4 isobutene; −2 bipyridine[b]	$-2H_2O$[c]		
$[Mn(dtbp)_2(bpy)_2 \cdot 2H_2O]_n$ (**4**)	60−110	110−300	400−700	74.1 (74.0)	$Mn(PO_3)_2$
$[Co(dtbp)_2(bpy)_2 \cdot 2H_2O]_n$ (**5**)	30−96	100−200	200−330	73.9 (73.7)	$Co(PO_3)_2$
$[Cd(dtbp)_2(bpy)_2 \cdot 2H_2O]_n$ (**6**)	60−110	110−275	275−700	69.5 (69.3)	$Cd(PO_3)_2$

[a] Loss of two water molecules. [b] Loss of four isobutene and two bipyridine molecules. [c] Loss of two more water molecules through P−OH condensation. [d] Value corresponds to the expected loss for formation of the metaphosphate material.

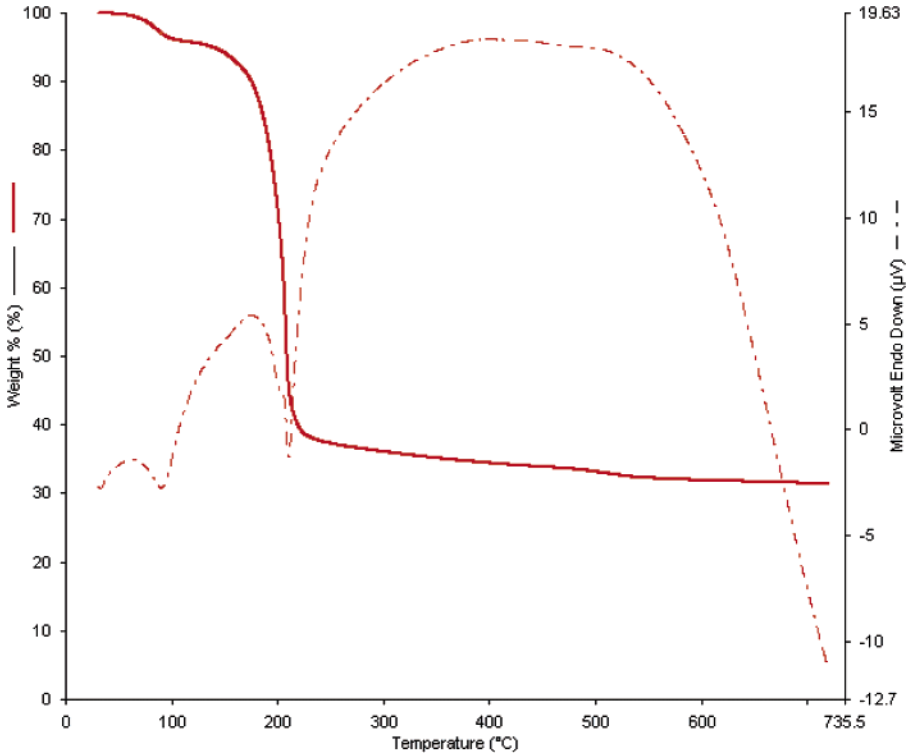

Figure 7. TGA−DTA trace for the thermal decomposition of $[Cd(dtbp)_2(bpy)_2 \cdot 2H_2O]_n$ (**6**) (scan rate 10 °C/min). The traces for compounds **4** and **5** are similar.

from methanol yielded an analytically pure compound. Anal. Calcd for $C_{36}H_{56}MnN_4O_{10}P_2$: C, 52.6; H, 6.9; N, 6.8. Found: C, 52.7; H, 6.9; N, 6.9. IR (KBr, cm^{-1}): 3493 (vs), 3282 (m), 3078 (m), 2973 (vs), 2927 (s), 1602 (vs), 1537 (s), 1490 (s), 1415 (s), 1391 (s), 1367 (s), 1250 (s), 1221 (s), 1196 (vs), 1081 (vs), 1038 (s), 1008 (s), 976 (vs), 915 (s), 823 (s), 733 (s), 705 (s). UV−vis (CH_3OH): 296 nm. TGA [temp range, °C (% weight loss)]: 60−100 (4.4); 100−205 (27.3); 205−430 (38.0); 430−600 (4.4). DSC (°C): 107 (endo); 208 (endo).

Conversion of 2 to 5. Polymer **2** (1 mmol) was dissolved in methanol (40 mL), and solid bipy (2 mmol) was added and stirred for a few hours. The resulting solution was filtered and kept at room temperature to yield **5** as single crystals in 79% yield.

Alternate Route for Synthesis of 5. A solution of 4,4′-bipyridine (624 mg, 4 mmol) in methanol (10 mL) was added to a methanol solution (50 mL) of cobalt acetate (540 mg, 2 mmol). Solid dtbp-H (840 mg, 4 mmol) was added to the above solution and stirred for 1 h. The resultant solution was filtered and kept for crystallization in a beaker at 15 °C. Single crystals of **5** were obtained after 48 h. Anal. Calcd for $C_{36}H_{56}N_4CoO_{10}P_2$: C, 52.4; H, 6.8; N, 6.8. Found: C, 52.1; H, 6.5; N, 7.2. IR (KBr, cm^{-1}): 3482 (br), 3105 (w), 3081 (m), 2978 (s), 2932 (m), 1604 (s), 1538 (m), 1489 (m), 1414 (m), 1366 (m), 1252 (m), 1197 (s), 1085 (vs), 1037 (m), 1008 (m), 974 (vs), 823 (m), 705 (m), 629 (m), 503 (m). TGA [temp range, °C (weight loss)]: 30−96 (4.4); 100−200 (65.0); 200−330 (4.3); 330−700 (8.6). DSC (°C): 50 (endo), 170 (endo); 195 (endo), 340 (endo).

Conversion of 3 to 6. Polymer **3** (1 mmol) was dissolved in methanol (40 mL), and solid 4,4′-bipy (2 mmol) was added and stirred for a few hours. The resulting solution was filtered and kept at room temperature to yield **6** as single crystals in 66% yield.

Alternate Route. A solution of 4,4′-bipyridine (624 mg, 4 mmol) in methanol (10 mL) was added to a methanol solution (50 mL) of cadmium acetate (540 mg, 2 mmol). Solid dtbp-H (840 mg, 4 mmol) was added to the above solution and stirred for 1 h. The resultant solution was filtered and kept for crystallization in a beaker at 15 °C. Single crystals of **6** were obtained after 48 h. Yield: 1.16 g (66%). Anal. Calcd for $C_{36}H_{56}CdN_4O_{10}P_2$: C, 49.2; H, 6.4; N, 6.4. Found: C, 49.3; H, 6.6; N, 6.5. IR (KBr, cm^{-1}): 3454 (br), 3280 (s), 3099 (s), 3072 (s), 3052 (s), 2973 (s), 2927 (s), 1603 (vs), 1536 (m), 1489 (s), 1417 (s), 1390 (s), 1366 (s), 1322 (s), 1252 (vs), 1223 (vs), 1187 (vs), 1076 (vs), 1038 (s), 1008 (vs), 976 (vs), 914 (s), 824 (vs), 733 (m), 706 (s), 688 (m), 629 (s), 579 (s), 544 (s), 504 (s), 467 (s). UV−vis (CH_3OH): 298 nm. ^1H NMR (CD_3OD, 300 MHz): δ 8.71 (d, $J_{H\alpha\alpha'} = 6$ Hz, 12 H), 7.84 (dd, $J_{H\beta\beta'} = 1.49$ Hz, 12 H), 1.42 (s, 36 H) ppm. ^{31}P NMR (CD_3OD, 121 MHz): δ 4.77 ppm.

Synthesis of $[(4,4'\text{-bpyH}_2)^{2+}(H_2PO_4)_2]_n$ (7). Route 1. 4,4′-Bipyridine (156 mg, 1 mmol), magnesium acetate (107 mg, 0.5 mmol), and dtbp-H (840 mg, 4 mmol) were dissolved in methanol

Table 7. Crystal Data and Structure Refinement for **2** and **4**−**7**

param	**2**	**4**	**5**	**6**	**7**
empirical formula	$C_{32}H_{72}Co_2O_{16}P_4$	$C_{36}H_{56}MnN_4O_{10}P_2$	$C_{36}H_{56}CoN_4O_{10}P_2$	$C_{36}H_{56}CdN_4O_{10}P_2$	$C_{10}H_{14}N_2O_8P_2$
fw	954.6	821.73	825.72	879.19	352.17
temp, K	93(2)	293(2)	133(2)	253(2)	133(2)
wavelength, Å	0.710 73	0.710 73	0.710 73	0.710 73	0.710 73
cryst system	monoclinic	monoclinic	monoclinic	monoclinic	monoclinic
space group	$P2_1/c$	$P2/c$	$P2/c$	$C2/c$	$P2_1/c$
a, Å	19.940(10)	15.9627(14)	15.846(3)	50.0409(10)	4.6740(1)
b, Å	13.286(6)	11.7157(12)	11.452(2)	11.7920(3)	18.036(8)
c, Å	17.739(6)	23.502(2)	23.008(5)	23.5506(5)	8.161(2)
b, deg	90.862(16)	92.783(8)	92.77(3)	106.073(3)	98.55(2)
V, Å^3	4699(4)	4390.1(7)	4170.3(15)	13353.6(5)	680.4(4)
Z; D_{calcd}, mg/m^3	4; 1.349	4; 1.243	4; 1.315	12; 1.312	2; 1.719
abs coeff, mm^{-1}	0.902	0.428	0.545	0.616	0.365
cryst size, mm^3	0.12 × 0.15 × 0.96	0.4 × 0.4 × 0.1	0.3 × 0.2 × 0.2	0.2 × 0.5 × 0.8	0.3 × 0.2 × 0.2
θ range, deg	1.84−30.47	1.28−24.99	1.77−24.75	0.85−28.51	2.26−24.67
data (params)	12 498 (511)	7703 (500)	7112 (482)	16 346 (802)	1157 (128)
GOOF on F^2	0.999	1.098	1.022	0.920	1.089
R1, wR_2 [I > 2σ(*I*)]	0.0473, 0.0992	0.0455, 0.1301	0.0954, 0.2337	0.0497, 0.1261	0.0258, 0.0656

(5 mL). Petroleum ether (5 mL) and water (5 mL) were added to the above solution and filtered into a test tube. The tube was sealed and heated at 80 °C. Colorless crystals of $[Mg(HPO_4)(H_2O)_3]$ (**8**) that formed at bottom of the tube after 72 h were collected on a filter paper by filtration, washed with water (2 × 10 mL), and air-dried. The filtrate was left for crystallization in a beaker at room temperature. Single crystals of $[(bipyH_2)(H_2PO_4)_2]$ were obtained after 48 h. Yield: 0.3 g (85.2%).

Route 2. The 4,4′-bpy (156 mg, 1 mmol) was dissolved in methanol (40 mL). To this solution, H_3PO_4 (230 mg (85% solution), 2 mmol) was added. The resulting turbid solution was heated on a water bath to make the solution clear. The clear solution was kept at room temperature for crystallization. X-ray-quality crystals were obtained from the same solution. Yield: 0.34 g (97%). Mp: 221−223 °C. Anal. Calcd for $C_{10}H_{14}N_2O_8P_2$: C, 34.1; H, 3.5; N, 8.0. Found: C, 34.2; H, 3.4; N, 7.8. IR (KBr, cm^{-1}): 3432 (b), 3114 (w), 3056 (w), 1633 (m), 1593 (w), 1489 (m), 1234 (m), 1119 (s), 978 (vs), 788 (s), 492 (m). UV−vis (CH_3OH; nm (ϵ, cm^{-1} M^{-1})): 290 (1789). ^{1}H NMR (CD_3OD, 400 MHz): δ 8.7 (d), 7.9 (d) ppm. ^{31}P NMR (CD_3OD, 121 MHz): δ 0.37 (s) ppm.

Characterization data for $[Mg(HPO_4)(H_2O)_3]$ (8). Anal. Calcd for MgH_7O_7P: C, 0.00; H, 3.17. Found: C, 0.00; H, 3.16. IR (KBr, cm^{-1}): 3514 (m), 3481 (m), 3397 (m), 3279 (m), 2921 (w), 1702 (m), 1653 (m), 1445 (m), 1239 (m), 1167 (s), 1062 (vs), 1022 (vs), 900 (m), 693 (m), 554 (w), 509 (w).

Solid-State Thermolysis of 4−6. Using the TGA data on samples **4**−**6**, the thermal decomposition studies of the bulk samples were carried out on a temperature-controlled furnace. In a typical experiment, 1 g of the respective sample was placed on a ceramic boat and heated in air initially at 600 °C for 48 h. The product obtained at this stage was characterized by elemental analysis and PXRD studies. If residual amounts of carbon and hydrogen were found in the materials, the original samples were once again heated at 700 °C to obtain the final materials.

Characterization Data for $Mn(PO_3)_2$ (9). Anal. Calcd for MnO_6P_2: C, 0.00; H, 0.00. Found: C, 0.00; H, 0.55. PXRD (Mo Kα): 2θ 4.33, 9.72, 11.98, 14.24, 19.01, 19.33, 20.63, 24.80, 25.95, 27.21, 27.72, 29.37, 30.56, 34.31, 37.04, 38.98, 40.56, 42.26, 50.71, 53.22, 55.21, 55.89, 58.75°.

Characterization Data for $Co(PO_3)_2$ (10). Anal. Calcd for CoO_6P_2: C, 0.00; H, 0.00. Found: C, 0.17; H, 0.00. PXRD (Mo Kα): 2θ 4.26, 10.92, 14.05, 14.81, 17.72, 19.82, 20.69, 21.30, 24.15, 24.46, 25.74, 26.90, 28.05, 28.54, 28.62, 30.20, 31.76, 35.34, 35.84, 36.87, 38.33, 40.00, 40.77, 41.97, 43.65, 45.40, 47.34, 49.73, 52.84, 53.54, 54.63, 57.00, 57.79, 59.07°.

Characterization Data for $Cd(PO_3)_2$ (11). Anal. Calcd for CdO_6P_2: C, 0.00; H, 0.00. Found: C, 0.18; H, 0.00. PXRD (Mo Kα): 2θ 5.88, 9.06, 12.17, 14.58, 15.96, 19.22, 19.52, 20.48, 21.34, 22.46, 23.23, 24.18, 25.04, 26.74, 27.47, 28.15, 28.98, 29.26, 30.12, 30.40, 30.87, 31.72, 33.04, 33.79, 34.50, 36.11, 36.83, 38.84, 39.36, 40.83, 41.78, 42.74, 44.56, 47.31, 49.34, 51.56, 52.46, 53.18, 53.67, 54.21, 55.42, 56.24, 57.66, 58.56°.

X-ray Structure Analysis. Single crystals of compounds **2** and **4**−**7**, suitable for X-ray structure analysis, were grown by using the procedures described vide supra. Single-crystal X-ray diffraction measurements were made on a STOE AED 2 diffractometer for **5**, and **7**, a Nonius MACH3 diffractometer for **4,** and a Bruker CCD system for **2** and **6**. All calculations were carried out using the programs in the WinGX model.[34] The structure solutions for all compounds were achieved using direct methods (SIR-92[35] or SHELXS-97[36]), and the structures were refined using SHELXL-97.[37] The positions of hydrogen atoms were geometrically fixed and refined using a riding model other than in the case of **7**, for which the H atom attached to oxygen and nitrogen were located from the difference map. All non-hydrogen atoms were refined anisotropically. The *tert*-butyl groups of the dtbp ligand found in the grid formed by Cd(2) in **6** are disordered due to high thermal motion. Other details of data collection, structure solution, and refinement are summarized in Table 7.

Acknowledgment. R.M. thanks the DST, New Delhi, India, for the support of this work through a Swarnajayanti Fellowship. The authors thank the DST-funded National Single Crystal X-ray Diffraction Facility at IIT-Bombay for the diffraction data of **4** and the SAIF, IIT-Bombay, for spectral data.

Supporting Information Available: Details of the X-ray crystal structure determinations of compounds **2** and **4**−**7** in the form of CIF files. This material is available free of charge via the Internet at http://pubs.acs.org.

IC050742Z

(34) WinGX, version: 1.64.05: Farrugia, L. J. *J. Appl. Crystallogr.* **1999**, *32*, 837.
(35) Altomare, A.; Cascarano, G.; Giacovazzo, C.; Gualardi, A. *J. Appl. Crystallogr.* **1993**, *26*, 343.
(36) Sheldrick, G. M. *SHELXS-97, Program for Structure Solution*; University of Göttingen: Göttingen, Germany, 1997.
(37) Sheldrick, G. M. *SHELXL-97, Program for Structure Refinement*; University of Göttingen: Göttingen, Germany, 1997.